Experimental Study of Anomalous Electron Stream Behavior*

M. H. MILLER AND W. G. DOW
Department of Electrical Engineering, The University of Michigan, Ann Arbor, Michigan
(Received February 8, 1960; and in final form October 27, 1960)

Experimental measurements on the characteristics of the sole current in a rectilinear crossed-field beam are reported. The sole current may be assigned a kinetic temperature on the order of 10 v corresponding to energy in excess of that corresponding to motion in static fields. The energy exchange leading to this excess energy is believed to be associated with multiple-loop trajectories in the low-potential region near the cathode.

I. INTRODUCTION

IT has been known for several years that electrons flowing in what are obstensibly static crossed-electric and magnetic fields could be collected by an electrode whose potential is considerably more negative than that of the cathode from which the electrons originate.[1-3] Superficially, this phenomenon implies a violation of energy conservation principles in that electrons are gaining energy in excess of that corresponding to motion in static fields. Explanations of this phenomenon in terms of such causes as contact difference of potential or initial thermal velocities are untenable because of the observed magnitude of the excess energy involved. If energy conservation principles are to be retained, the explanation of this phenomenon must involve a mechanism whereby electrons exchange energy with one another in the course of their motion. It has been suggested that this mechanism is a crossed-field slipping-stream amplification process, the so-called diocotron effect. However, the energy exchange predicted on this basis is of too small a magnitude to account for the experimental observations. While the actual mechanism should be generically related to the diocotron effect, the details of the mechanism must be significantly different.

The investigation reported in the following was undertaken as a part of a general study of the energy-exchange mechanism in order to extend the available experimental information about the phenomenon.

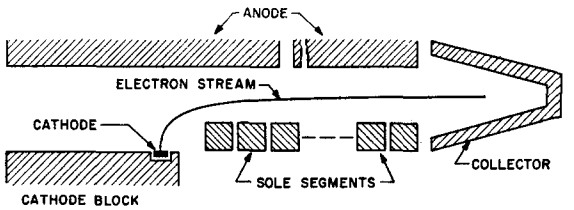

FIG. 1. Crossed-field stream analyzer geometry.

II. CROSSED-FIELD STREAM ANALYZER

Figure 1 is a sketch illustrating the geometry of a crossed-field stream analyzer constructed to observe and measure the energy-exchange phenomenon. The structure is basically that of a linear magnetron amplifier modified to suit the purposes of the present investigation. The plate is a smooth electrode in that it does not form a slow-wave structure; actually it consists of four segments electrically insulated from one another. The sole is divided into 31 electrically insulated segments each of which is 0.10 in. wide and spaced from its neighbors by 0.020 in. The spacing between the anode and the sole is 0.20 in. Figure 2(a) is a photograph of the cross section of the stream analyzer prior to assembly (only one sole segment is in place). The two side supports shown in the photograph (numbered 1 and 2) are hot-rolled steel magnetic pole pieces used in creating the crossed-field environment. Figure 2(b) is a photograph of the assembled sole structure with the side supports removed to expose the view. Also shown in the photograph, mounted to the right of the sole segments, is the cathode assembly. The cathode is a directly heated tungsten tape 0.040 in. wide which is mounted in a notch milled into a copper block. The electron gun is a modification of a conventional crossed-field gun based on the injection of a single electron into the plate-sole space along a cycloidal trajectory. Figure 3 is a photograph of the stream analyzer mounted in an electromagnet and connected to the measuring circuitry used.

III. SPACE-CHARGE-FREE ELECTRON TRAJECTORIES

The nature of the stream-analyzer construction did not permit visual observation of the electron-stream trajectory. Both intuition and the measurements to be described suggested a knowledge of the stream trajectory to be of importance. Hence, to provide a measure of the actual stream trajectory, the trajectory of a single electron in the stream-analyzer geometry was studied under varying conditions of magnetic field and electrode potentials. The general character of an electron trajectory in the main part of the plate-sole space, where essentially uniform field conditions prevail, is that of various types of trochoids. The details of this portion of the trajectory depend on the manner in which the electron is injected into the plate-sole space, in

* Submitted in partial fulfillment of the requirements for the Ph.D. degree at the University of Michigan, Ann Arbor, Michigan. This work was carried out in the Electron Physics Laboratory and was supported by the U. S. Army Signal Research and Development Laboratory.

[1] H. Alfven, L. Lindberg, K. G. Malfors, T. Wallmark, and E. Astrom, Trans. Roy. Inst. Technol. Stockholm (1948).

[2] R. Warnecke, H. Huber, P. Guenard, and O. Doehler, Compt. rend. **235**, 470 (1952).

[3] P. Guenard and H. Huber, Ann. Radioélec. **7**, 252 (1952).

particular, on the nature of the trajectory in the vicinity of the cathode and first sole segment. The trajectory in this region is particularly important because the experimental measurements showed that it is in this region that the principal energy exchange occurs.

The nature of the trajectories[4] in the cathode region was calculated for various values of magnetic field and electrode potentials using a differential analyzer. A conducting film analog of the stream-analyzer geometry was constructed and information on the electric-field components and potential, extracted from the analog by means of a four-contact traveling probe, was fed into a computer programmed with the equations of motion of an electron normal to a uniform magnetic field. The computer output (coordinate position of the electron) controlled the movement of the probe. An auxiliary recorder duplicated the probe motion to form a permanent record. The general nature of the trajectories plotted is sketched in Fig. 4. The dotted lines in this figure illustrate the general configuration of the equipotential contours. The curve denoted by A represents the generally smooth injection into the plate-sole space obtained with relatively low magnetic fields. As the magnetic field is increased the electron is forced to pass through a region of steeply sloping equipotential contours (curve B). Because the potentials along this trajectory are lower than those corresponding to the A trajectory, characteristic trochoidal loops appear and the transit time from the cathode into the plate-sole space is increased. For relatively high magnetic fields an electron trajectory such as that illustrated by curve C is obtained. The electron executes many trochoidlike loops in following, approximately, a potential contour which dips down into the gap between the cathode block and the first sole segment. The transit time for such a trajectory becomes extremely long (in one case, with 800 v between anode and cathode, the average velocity in the gap corresponded to somewhat more than 1 ev).

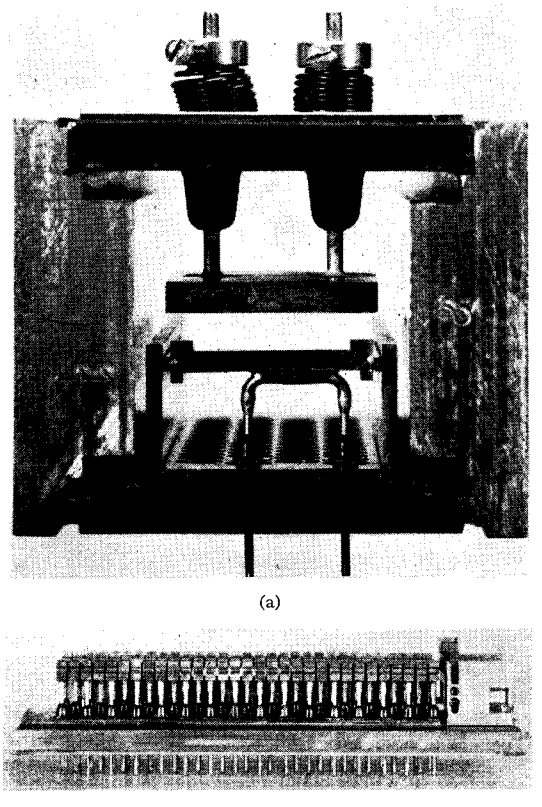

(a)

(b)

FIG. 2. (a). Stream analyzer cross section. (b). Sole assembly.

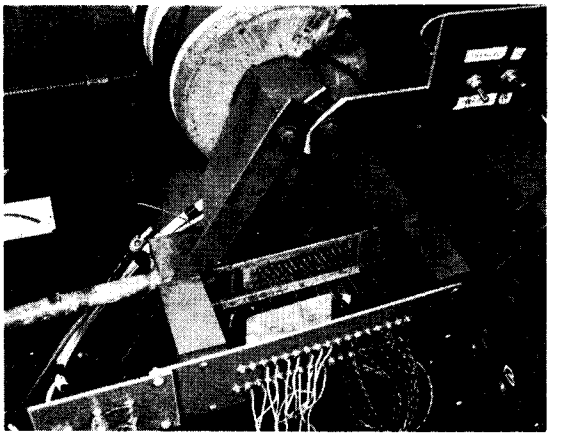

FIG. 3. Experimental test setup.

IV. EXPERIMENTAL MEASUREMENTS

A. Preliminary Measurements

Preliminary measurements were made, more or less at random, to establish the existence of the energy-exchange phenomenon in the stream analyzer and to determine the general range of parameters (voltage, current, and magnetic field) over which it occurred. With this information as a guide, data were obtained on the gross nature of the negative-sole-current phenomenon.[5] Figure 5 is a plot of the experimental volt-ampere relation for the electron gun and shows the range of parameters over which data were taken (ϕ_{0A} is the anode-cathode potential, ϕ_{0s} is the sole-cathode potential, I_{0k} is the cathode current, B_0 is the magnetic-field strength). Also plotted in this figure for comparison is the theoretical limiting volt-ampere characteristic for zero magnetic field, calculated on the basis of the gun geometry being approximately that of a parallel-plane diode. As the data indicate, the cathode was operated under space-charge limited conditions.

[4] M. H. Miller, The University of Michigan, Electron Physics Laboratory, Electrical Engineering Department Tech. Rept. No. 26 (July, 1958).

[5] In the course of taking data, failure of the vacuum pump caused a loss of the filament. While the nominal dimensions of the replacement parts were the same as the original, it was not possible to duplicate the original geometry exactly. To differentiate data taken with the original cathode from those taken with the replacement assembly, the former are labeled "cathode No. 1" and the latter, "cathode No. 2."

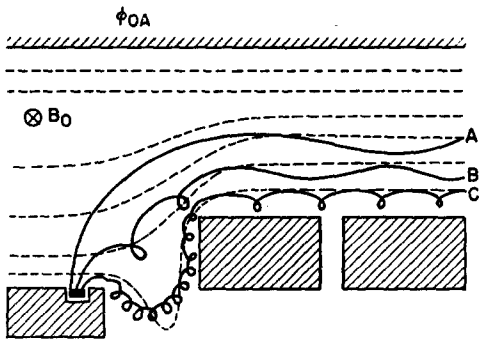

FIG. 4. Space-charge-free trajectories.

While the measured volt-ampere characteristics are quite closely linear, all the characteristics must eventually become asymptotic to the limiting characteristic for zero magnetic field, as the anode potential is increased. However, over the range of measurements, the beam perveance $I_{0k}/\phi_{0A}^{\frac{3}{2}}$ is simply proportional to the square root of the factor ϕ_{0A}/B_0^2.

The dependence on the parameter ϕ_{0A}/B_0^2 is not accidental; it can be shown that in any given geometry the beam perveance is in general a function of only the ratio of the electrode potentials to the square of the magnetic-field strength.[6]

Since the scaling parameter ϕ_{0A}/B_0^2 is a significant one in subsequent discussion, it is pertinent to state certain of its properties. If the ratio of electrode potential to the square of magnetic field is held constant in a given electrode geometry, the geometry of the trajectory traced by an electron is independent of the particular choice of electrode potential and magnetic field used to obtain a given value of scaling parameter. However, the time for an electron to trace out a given portion of its trajectory varies inversely with magnetic-field strength.

Data were taken which show that the energy-exchange phenomenon scales with the parameter ϕ_{0A}/B_0^2. Figure 6 is a plot of the fraction of the cathode current collected by the sole (I_{0s}/I_{0k}) as a function of the scaling parameter ϕ_{0A}/B_0^2. A wide range of voltage and currents was used to obtain these data so as to illustrate the validity of the scaling parameter as a measure of the energy-exchange phenomenon. Figure 7 shows the same type of data, taken with cathode No. 2, for three scalings of the sole potential (sole potential negative relative to cathode). For the measurements described by both Figs. 6 and 7 there was no observed anode current, i.e., the cathode current was collected either by the sole or by the collector after the stream

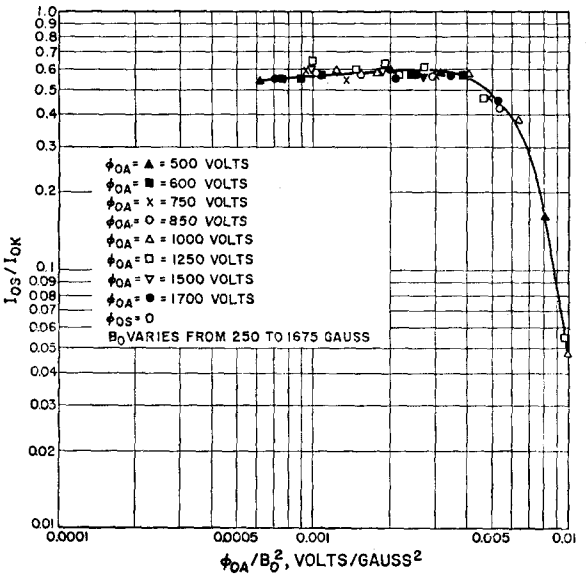

FIG. 6. Gross sole current characteristic, cathode No. 1.

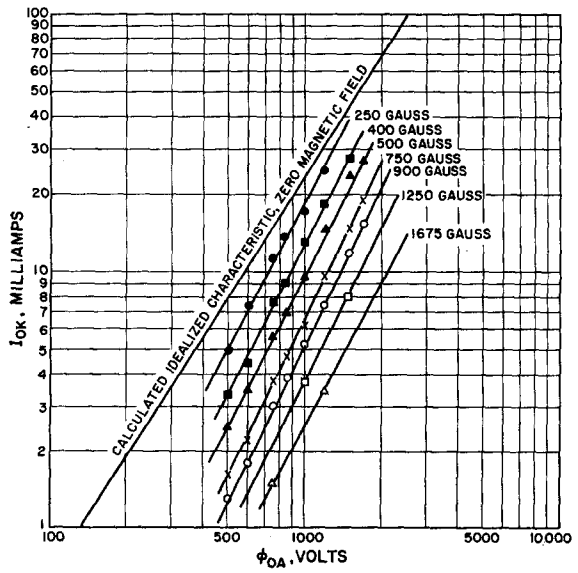

FIG. 5. Volt-ampere characteristic of the stream-analyzer gun.

had left the plate-sole space. For future reference it will be noted here that the space-charge free-trajectory computations described in Sec. III indicated a change from the C to the B type of trajectory (Fig. 4) at a value of the scaling parameter corresponding to the sharp dropoff in sole current.

B. Distribution of Negative-Sole Current Along the Sole

Measurements were made of the distribution of current collected by the sole as a function of distance along the sole. These measurements were made in the following fashion: (1) For a given measurement, the stream analyzer was operated at a fixed value of the scaling parameter, i.e., at a fixed anode potential and magnetic field. (2) The sole was held at a fixed potential and the currents to all the electrodes were measured. The current to each sole segment was measured separ-

[6] J. R. Pierce, *Theory and Design of Electron Beams* (D. Van Nostrand Company, Inc., Princeton, New Jersey, 1954), pp. 16–18.

ately. Measurements were made for a number of values of sole potential for each value of scaling parameter. (3) The measurements just described were made over the range of values of scaling parameter which the preliminary measurements had shown to be significant.

It is convenient to present the data in the form of an integrated distribution curve, i.e., as a plot of I_{0tn}/I_{0k} against distance along the sole. I_{0tn} is the direct current remaining in the stream *after* it has passed over the nth sole segment and *before* it passes over the $(n+1)$th sole segment. Distance along the sole is measured in terms of the period of the sole segmentation (probe unit=0.12 in.). The edge of the sole nearest the cathode is taken as the origin. Figures 8, 9, and 10 are representative of the data obtained. For all the data there was no anode current. The cathode current was collected either by the sole, or after it had passed completely through the plate-sole space.

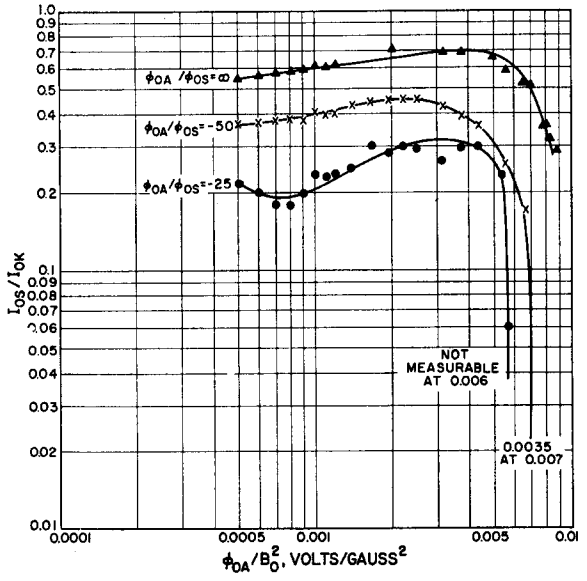

FIG. 7. Gross sole current characteristic, cathode No. 2.

One interesting characteristic of the data is the sizeable fraction of the total sole current which is collected by the first few sole segments. Indeed, a significant fraction of the total sole current is collected on the first sole segment alone. These data suggest that the energy-exchange process, through which electrons gain the added energy necessary to reach a negatively biased sole, manifests itself before the beam enters the plate-sole space.

C. Energy Distribution in the Negative-Sole Current

The energy distribution in the stream as it passed over a given sole segment was sampled by using the sole segments as probes. Measurements were taken of current to the several sole segments as a function of the potential of one sole segment, all other potentials and

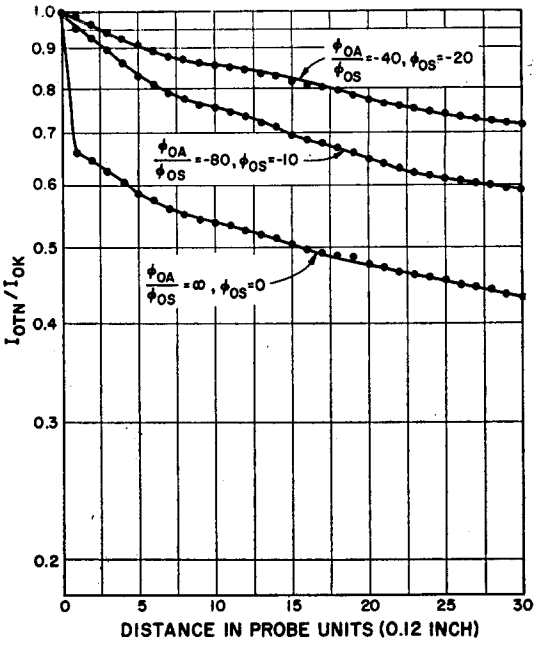

FIG. 8. Distribution of sole current along the sole. ($\phi_{0A}=-800$ v, $B_0=1000$ gauss, $\phi_{0A}/B_0^2=0.8\times10^{-3}$ v/gauss^2; cathode No. 2.)

the magnetic field remaining fixed. Figure 11 is typical of the data obtained. For these particular data the potential of the seventh sole segment (from the cathode) was varied. In addition to plotting the current to a number of sole segments in Fig. 11, the total sole current I_{0s} is also plotted. It is interesting to note that the variation of potential of the probe segment affected only the division of current between sole segments and not the total amount of current collected by the sole.

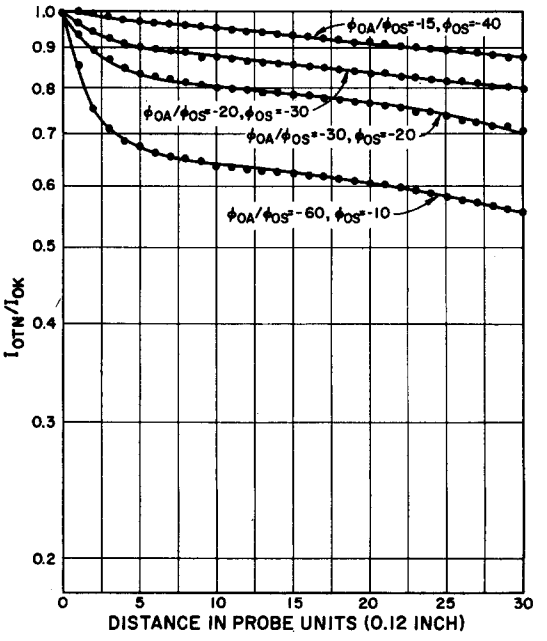

FIG. 9. Distribution of sole current along the sole. ($\phi_{0A}=600$ v, $B_0=500$ gauss, $\phi_{0A}/B_0^2=2.4\times10^{-3}$ v/gauss^2; cathode No. 2.)

It is also interesting that the currents to sole segments before the seventh segment are insensitive to the probe potential. The relatively small slope of the current characteristic of the sixth segment can be attributed to the distortion of the potential contours in the vicinity of the seventh sole segment.

Figure 12 illustrates the nature of the probe characteristics taken as a function of distance along the sole. Measurements were made in the manner described in the foregoing for the same potentials and magnetic field as were used to obtain the data presented in Fig. 11, except that different sole segments were used, in turn, as probes.

Measurements similar to the foregoing energy distribution measurements were taken in the following manner: for fixed operating conditions the potential of the forth sole segment was set at a given value (not, in general, the same as ϕ_{0s}), and the current to the seventh sole segment was measured as a function of the potential of the seventh segment. This measurement was made for several different potentials of the fourth sole segment. Typical data obtained are shown in Fig. 13.

It can be noted that when the current to the fourth probe is increased (by making ϕ_{0s4} less negative), there is a consequent reduction of the current to the seventh probe. On the other hand, if the fourth probe is made sufficiently negative so that it no longer collects a significant amount of current, then a further decrease in its potential has little effect at the seventh probe.

The approximate linearity of the plotted probe characteristic indicates that the energy distribution among the electrons collected by a probe is approximately Maxwellian. It is convenient, therefore, to

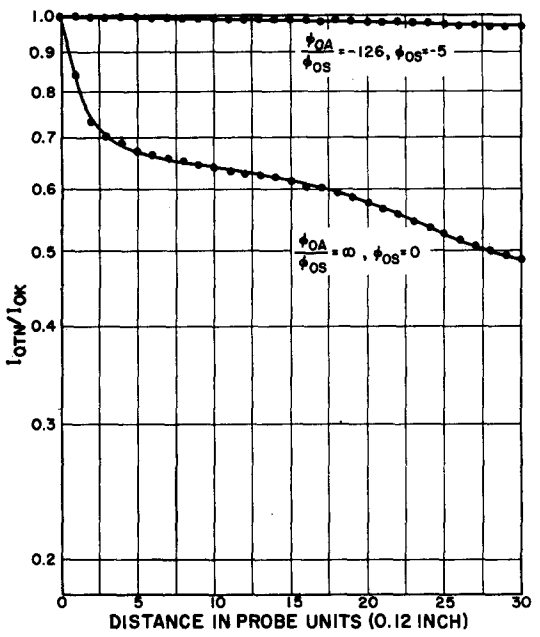

FIG. 10. Distribution of sole current along the sole. ($\phi_{0A}=630$ v, $B_0=300$ gauss, $\phi_{0A}/B_0^2=7.0\times10^{-3}$ v/gauss^2; cathode No. 2.)

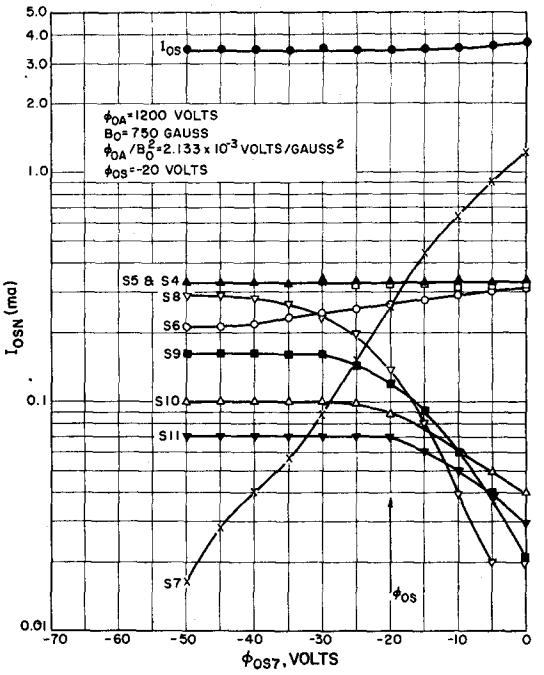

FIG. 11. Energy distribution curves, sole segment No. 7 (cathode No. 1).

ascribe a temperature to the probe current, measured from the slope of the characteristic, which describes the average energy of the probe current. The kinetic temperature corresponding to the data presented in Fig. 11 is approximately 11 ev.

The linearity of the probe characteristics also suggests that the energy distribution in the beam is also approximately Maxwellian. However, electron trajectories in the beam are in general trochoidal, and therefore electrons approach a probe with a wide range of normal and tangential velocity components. It is, therefore, questionable as to whether all electrons with an energy higher than that necessary for collection by a negatively biased probe will actually be collected by a probe.

There are, nevertheless, several reasons supporting the belief that the probe measurements do reflect the energy distribution in the beam (energy in excess of that corresponding to conservative motion).

It will be noted that electrons which gain excess energy consequently experience an increased magnetic force which causes them to move closer to the sole. They are therefore more favorably disposed toward collection by a sole probe. In this respect it can also be noted that the period of the trochoidal motion of the electrons is, over the range of the measurements, of the same order of magnitude as the period of the sole segmentation. For the data shown in Fig. 11, for example, the trochoidal period is about half the sole period. The width of the probes is hence not too small to properly sample the beam.

Data such as those shown in Fig. 11 also support the

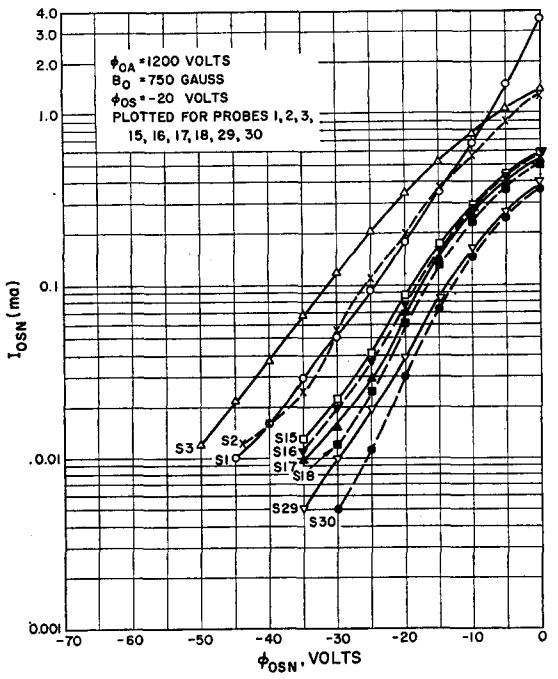

FIG. 12. Energy distribution curves, sole segments 1, 2, 3, 15, 16, 17, 18, 29, 30 (cathode No. 1).

assertion that the probes measure the beam energy. The fact that the probe potential does not significantly affect the total sole current, but rather only the division of current between various sole segments, suggests that essentially all the electrons which have sufficient energy to reach the sole actually do so.

D. Radio-Frequency

During the repair of the cathode assembly, mentioned previously, advantage was taken of the opportunity to insert a coaxial electric probe in the region immediately back of the filament. Weak rf signals were detected in the range of values of the scaling parameter corresponding to high sole current. Depending on particular operating conditions, the frequency of the observed signals was in the range of 2 to 3 kMc. It was noted that the frequency of the observed signal was sensitive to the potential on the first, and only the first, sole segment. It was also noted that the introduction of a 1-w signal (from an external generator) of approximately the same frequency as that emanating from the stream analyzer would cause large variations in the negative-sole current. Depending on the frequency of the applied signal (over about a 100-Mc range) the negative-sole current could be increased or decreased, about the value of sole current for no applied signal.

The frequency spectrum of the observed signal was investigated by displaying it on a spectrum analyzer after amplification by a traveling-wave tube. Figure 14 shows photographs of a typical spectrum obtained. The two photographs shown are of the same spectrum, with the sweep speed for the first photograph adjusted to obtain a steady pattern, and with a single sweep for the second photograph. It is interesting to note that the observed signal is a coherent one.

V. INTERPRETATION OF THE DATA

It was at least intuitively evident that the sole-current phenomenon was associated with the character of the electron stream rather than with the rf properties of the electrode structure; i.e., because of the relatively low electron velocities involved it seemed unlikely that any significant coupling would exist with rf waves which could be supported by the electrode structure. This conclusion is supported by the initial measurements which established the scalability of the phenomenon. For each particular value of scaling parameter the electron trajectories are fixed for a given electrode geometry. The time scale, i.e., the velocity of the electron motion, varies, however, depending on the particular choice of magnetic field used to obtain a given value of the scaling parameter. Since the sole-current phenomenon is scalable, the coupling between the rf properties of the structure and the beam is negligibly dependent on the time scale, and therefore on frequency. This conclusion is difficult to accept unless the coupling itself is negligible.

The scalability of the phenomenon also indicates that the shape of the electron trajectories is a very important consideration in evaluating the experimental data. One is thus led into examining the sole-current measurements for any correlation with the computed electron trajectories.

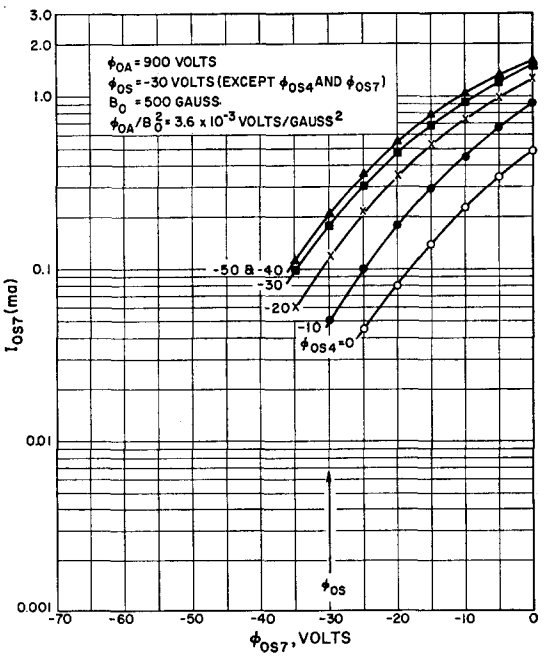

FIG. 13. Energy distribution curves, sole segment No. 7 (cathode No. 2).

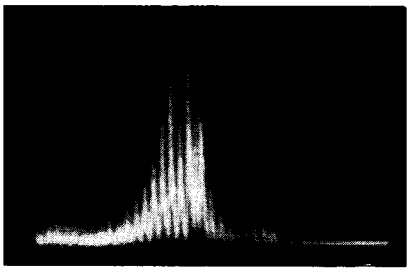

(a)

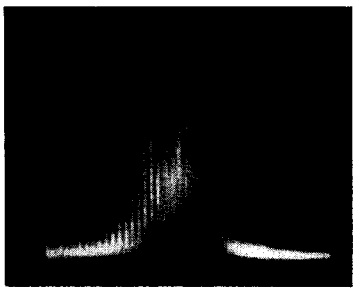

(b)

FIG. 14. Spectrum of observed rf signal. $\phi_{0A}=700$ v, $\phi_{0s}=-35.5$ v, $B_0=500$ gauss, $\phi_{0A}/B_0^2=2.8\times10^{-3}$ v/gauss^2. (a) Synchronized sweep; (b) Single sweep.

It was noted that the gross sole current falls off steeply at about the same value of scaling parameter at which the computed electron trajectories dip down into the low-potential well between the cathode and the first sole segment. Of course, the computed trajectories are calculated neglecting space-charge forces, and there is a question as to how well they correspond to actual trajectories. However, the space-charge forces will be relatively small for the low current densities used in obtaining data provided electrons pass rather quickly from the cathode into the plate-sole region. Therefore, the space-charge free computations should demarcate fairly well the value of scaling parameter for which electron trajectories begin to change from those corresponding to a rapid transit into the plate-sole space to long transit time trajectories passing through the low-potential well. In any event, a correlation between electron trajectories and sole current is only suggested and not evidenced by comparing the computations with the data.

On the other hand, there is definite evidence that the energy-exchange mechanism is associated with the character of the electron stream in the neighborhood of the cathode block. The fact that a major fraction of the sole current is collected on the first few segments indicates that the energy exchange necessary for the collection has already been accomplished at the beginning of the plate-sole space.

The data showing the distribution of sole current along the sole indicate a relatively sharp change in slope of the curves at about the first third of the sole. The implication that can be drawn from these data is that the energy-exchange mechanism is not particularly effective in the latter part of the plate-sole region. Further, since the plate-sole region is more or less uniform in geometry, it seems unlikely that the energy-exchange mechanism would be more effective toward the beginning of the sole than toward the end of the sole. Therefore it would appear that the near vicinity of the cathode is again indicated as the location of the principal energy exchange.

This is not to say that there is no energy exchange at all in the plate-sole space. As stated previously, the period of the trochoidal motion of the electrons is, over the range of the measurements, of the same order of magnitude as the period of the sole segmentation. Hence, if the energy exchange took place entirely in the neighborhood of the cathode block, all the electrons collected by the sole would be collected on the first few segments. The fact that some current is collected by all the segments indicates that some energy exchange occurs in the plate-sole space. However, since the amount of current collected tapers off rapidly along the sole, this energy exchange is small. It seems likely that the current to the sole segments toward the end of the sole comes from electrons which have not quite gained enough energy in the cathode region to be able to reach the sole, and which gain the necessary additional energy from a relatively small energy exchange in the plate-sole space.

Further evidence that the phenomenon occurs in the neighborhood of the cathode is found in data such as those shown in Fig. 11. Variation of the potential of one sole segment affected only the distribution of current along the sole without altering the gross sole current. Further, except for an explainable small change in current to the preceding segment, only the currents to segments succeeding the one whose potential was being varied were affected. The implication of these data is again that we are dealing with an energy exchange already substantially accomplished by the time the stream is in the plate-sole space.

For still another indication that the cathode region is, so to speak, the "home" of the energy-exchange phenomenon one can turn to the rf measurements. In particular, the sensitivity of the observed rf signal to the potential of the first, and only the first, sole segment can be noted. This sensitivity also supports the correlation between sole current and electron trajectories passing through the low potential region between the cathode and first sole segment. The potential contours in this region are quite sensitive to the potential on the first sole segment. We are led to the general hypothesis that the energy-exchange phenomenon is associated with multiple-loop trajectories in the low potential region between the cathode and the first sole segment. In this region the electron stream is in many respects analogous to an ion-neutralized electron gas. Space-charge forces are neutralized by the balancing action of electric and magnetic focusing fields rather than by a superposition of electric forces. Since the forward

velocity of the stream in this region is quite small, the balancing is roughly uniform across the stream. An electronic plasma of this sort would have a natural oscillation frequency about equal to the square root of the sum of the squares of the cyclotron and plasma frequencies. If this frequency is near resonance with the rotational component of the average electron motion a rather effective energy exchange can occur. Estimates of this frequency are of the same order of magnitude as the frequency of the experimentally observed signal.

It should be noted that the low potential region is not essential to the energy-exchange mechanism. It is only one means of causing turbulence in an electron stream and setting up conditions for a resonance between the dc cyclotron motion of the electrons and an rf perturbation propagating on the beam as a whole.

JOURNAL OF APPLIED PHYSICS VOLUME 32, NUMBER 2 FEBRUARY, 1961

Note on Ferromagnetic Relaxation Equations

H. SUHL AND R. C. FLETCHER
Bell Telephone Laboratories, Inc., Murray Hill, New Jersey
(Received September 7, 1960)

An amplitude formulation is employed for determining the motion of the electron spins in a ferromagnetic insulator in the presence of scattering from inhomogeneities. This formulation justifies the omission of an explicit back reaction term in previous "energy" and "number of quanta" formulations in the usual case where a large number of spin waves are excited by the scattering centers. The excited spin waves add up in such an incoherent fashion that they do not react back on the principal mode.

THE equations determining the motion of the electron spins in a ferromagnetic insulator in the presence of scattering from inhomogeneities[1] have been formulated in two different ways leading to essentially the same results. Callen starts with the equations connecting the destruction of main precession quanta n_0, and the creation of spin mode quanta n', and/or phonons[2]:

$$\dot{n}_0 = -(\lambda_{0\sigma}+\lambda_{0k})n_0 \tag{1}$$

$$\dot{n}' = \lambda_{0k}n_0 - \lambda_{k\sigma}(n'-n_T'), \tag{2}$$

where n_T' is the number of spin wave quanta in thermal equilibrium and $\lambda_{0\sigma}$, λ_{0k}, and $\lambda_{k\sigma}$ are the characteristic coupling constants of the process. Fletcher, LeCraw, and Spencer use an energy balance representation connecting the energy in the main precession, W_0, with the energies in the spin modes, W_k[3]:

$$\dot{W}_0 = P-(W_0/T_{10})-\Sigma_k(W_0/T_{2k}) \tag{3}$$

$$\dot{W}_k = (W_0/T_{2k})-(W_k/T_{1k}), \tag{4}$$

where T_{10}, T_{2k}, and T_{1k} are equivalent coupling constants to $\lambda_{0\sigma}$, λ_{0k}, and $\lambda_{k\sigma}$ expressed as relaxation times, and P is the power absorbed from an applied alternating magnetic field.

Neither of these formulations contains a term allowing for a back reaction of the spin modes on the main precession. The question that naturally occurs is whether there are combinations of coupling constants for which the spin modes would have large enough amplitudes to require such a term. For instance, Seiden[4] has attempted to rectify this omission by adding a term $\lambda_{k0}(n'-n_T')$ to the first of Callen's equations and subtracting it from the second. It is the purpose of the present note to formulate these equations in still a third fashion in order to investigate the validity of this back reaction term.

The weakness of both of these formulations is that the phases of the modes of oscillation are neglected. We will use the complex amplitude method employed previously in investigating linewidth[1] and saturation effects.[5,6] The basic low-level equations relating the amplitude of the main precession a_0 (see the notation in footnote 5), with the amplitude of the kth spin mode b_k can be written

$$\dot{a}_0 = (i\omega_0-\eta_0)a_0+i\Sigma\nu_{0k}b_k+he^{i\omega t} \tag{5}$$

$$\dot{b}_k = (i\omega_k-\eta_k)b_k+i\nu_{k0}a_0, \tag{6}$$

where h is the amplitude of the circularly polarized applied rf magnetic field of frequency ω; $\nu_{0k}=\nu_{k0}^*$ is the scattering parameter coupling a_0 to b_k; and ω_0, η_0, ω_k, η_k are the resonance frequency and rate of loss to the lattice of the main precession and spin modes, respectively.

Note that the issue of the back reaction term does not arise in these equations since the time rate of change of amplitude of each mode is proportional to the amplitude

[1] A. M. Clogston, H. Suhl, and L. R. Walker, J. Phys. Chem. Solids **1**, 129 (1956).
[2] H. B. Callen, J. Phys. Chem. Solids **4**, 256 (1958).
[3] R. C. Fletcher, R. C. LeCraw, and E. G. Spencer, Phys. Rev. **117**, 955 (1960).
[4] P. E. Seiden, Compt. rend. **250**, 2530 (1960).
[5] H. Suhl, J. Phys. Chem. Solids **1**, 209 (1957).
[6] H. Suhl, J. Appl. Phys. **30**, 1961 (1959).